Model Assisted Statistics and Applications 6 (2011) 357–368
DOI 10.3233/MAS-2011-0192
IOS Press

Teaching Statistics

Time series modelling of maximum tsunami wave heights recorded in Sibolga (Sumatra)

S.S. De*, Goutami Chattopadhyay, Suman Paul and D. De
S.K. Mitra Centre for Research in Space Environment Centre of Advanced Study in Radio Physics and Electronics, University of Calcutta 1, Girish Vidyaratna Lane, Kolkata- 700 009, India

Abstract. This study reports univariate modeling methodologies applied to the maximum tsunami wave height over Sibolga, Sumatra. The univariate time series models fitted are autoregressive model (AR), autoregressive integrated moving average (ARIMA) and autoregressive neural network (AR-NN). Goodness of fit of the models to the time series of maximum tsunami wave height has been assessed using percentage of prediction error, Pearson correlation coefficient, and Willmott's indices. After rigorous skill assessment using the above three models, the AR-NN model with seven previous values as predictor has been identified as the best predictive model for the time series under study.

Keywords: Maximum tsunami wave height, AR, ARIMA, AR-NN, Sibolga

1. Introduction

The 26 December 2004 Sumatra–Andaman earthquake was the first $M > 9$ event to be recorded by a global network of broadband seismic stations and regional Global Positioning System (GPS) networks. Analysis of this data has led to a new understanding of the mechanics of great subduction zone of earthquakes [12]. Kinematic rupture models for the 2004 Sumatra–Andaman earthquake exhibit complexity on broad scales in both space and time [2,28]. Tsunamis are generated when the sea floor abruptly deforms and vertically displaces the overlying water. Tectonic earthquakes are associated with the earth's crust deformation. When these earthquakes occur beneath the sea, the water above the deformed area is displaced from its equilibrium position [15,27]. Waves are formed as the displaced water mass moves under the influence of gravity to regain its equilibrium. A tsunami is made up of a series of very long waves. The waves will travel outward on the surface of the ocean in all directions away from the source area, much like the ripples caused by throwing a rock into a pond. The wavelength and period of the tsunami waves will depend on the generating mechanism and the dimensions of the source event. If the tsunami is generated from a large earthquake over a large area, its initial wavelength and period will be greater. If a local landslide causes the tsunami, both its initial wavelength and period will be shorter. The period of the tsunami waves may range from 5 to 90 minutes. A tsunami can cause damage thousands of miles from its origin, so there may be several hours between its creation and its impact on the coast, more time than it takes for seismic waves to arrive. Works are also published earlier with different issues associated with tsunamis [19,29].

The tsunami event under consideration occurred at 07:59 local time (00:59 UTC) on 26 December 2004, a moment magnitude (Mw) 9.3 megathrust earthquake occurred along 1300 km of the oceanic subduction zone located 100 km west of Sumatra and the Nicobar and Andaman Islands in the eastern Indian Ocean [28]. Highly destructive waves were generated by up to about 10 m vertical displacements associated with massive (more than 20 m horizontally),

*Corresponding author: S.S. De, E-mail: de_syam_sundar@yahoo.co.in.

ISSN 1574-1699/11/$27.50

sudden movements of adjacent plates during this event. The catastrophic regional impact of this tsunami was tremendous. The presentation of the time series of tsunami wave heights for the December 2004 event are given over the major water basins of the Atlantic, Indian and Pacific oceans [28]. Those time series plots exhibited how the tsunami wave heights depart from the ordinary wave heights. Some typical measurements of tsunami heights along the different coastal lines of Sri Lanka have been reported [32]. Tsuji et al. surveyed the waveforms of the aforementioned event and reported that all of the recorded tsunami waveforms indicate subsiding sea level with duration of 30 to 60 minutes, followed by the rising up [30]. The surveys of this catastrophe include the works of Satake et al. [25]. The largest measured tsunami heights, which were at Lhoknga in northwest Sumatra about 15 km southwest of Banda Aceh, were greater than 30 m. Tsunami height decreased to about 1.5 m at Meulaboh, which is located in northwestern Sumatra about 175 km southeast of Banda Aceh. Tsunami heights of about 2 m were measured in Sibolga, a fishing port in a natural embayment about 500 km southwest of Banda Aceh [16].

It has been established by Saxena and Zielinski that maximum tsunami wave height and its direction of propagation will be an added parameter to the tsunami warning system [25]. Some significant papers in the literature are available, where various aspects of maximum tsunami wave heights have been studied statistically. A theoretical study was carried out by Mofjeld et al. to understand how the probability distribution for maximum wave heights during tsunamis depends on the initial tsunami amplitude and the tides [18]. Tang et al. carried out a wavelet analysis of the maximum wave heights [26]. The purpose of the present paper is to develop a univariate model for the maximum tsunami wave height. It has been attempted to examine whether a series of maximum wave heights observations can be modeled using a univariate approach. As the study zone, we have chosen Sibolga, which was affected by the devastating tsunami of 2004. For development of a complete forecast model, we need to test this approach for various other tsunami cases. The present paper is the first step.

The present paper deals with a time series of tsunami maximum wave heights over Sibolga obtained at 10-minute intervals. A detailed geographical description of the study area is available in Puspito and Gunawan, where a comprehensive survey of the tsunami wave height has been presented [22]. Since the wave height is the prime reason behind this catastrophe, it was felt that a study of the univariate time series might give some insight into its evolution. To do this, the autocorrelation structure of the time series would be analyzed at the outset and subsequently, the autoregressive modeling would be done using three methods: autoregression (AR), autoregressive integrated moving average (ARIMA), and autoregressive neural network (AR-NN). Section 2 discusses the autocorrelation structure of the time series, Section 3 discusses the implementation procedure of the three competing univariate models, Section 4 discusses the statistical skill assessment of the models, and Section 5 presents the conclusion.

2. Analysis of the autocorrelation function

The prefix "auto" in autocorrelation denotes the correlation of a variable with itself, so that temporal autocorrelation indicates the correlation of a variable with its own future and past values. In this sense, it provides information on data memory. For instance, a fast decrease is indicative of no correlated measurements. However, it may also be used to reveal periodicities in the data [21]. Sometimes such correlations are referred to as lagged correlations. Almost always, autocorrelations are computed as Pearson product-moment correlation coefficients, although there is no reason why other forms of lagged correlation cannot be computed as well [33]. Autocorrelation coefficients are for the present and past of a time series. It is mathematically defined as [33]:

$$r_k = \frac{\sum_{i=1}^{n-k} \left[(x_i - \bar{x}_-)\,(x_{i+k} - \bar{x}_+) \right]}{\left[\sum_{i=1}^{n-k} (x_i - \bar{x}_-)^2 \sum_{i=k+1}^{n} (x_i - \bar{x}_+)^2 \right]^{1/2}}$$

Where, r_k = autocorrelation coefficient of Lag k

$\bar{x}_-$ = First (n−k) data values

$\bar{x}_+$ = Last (n−k) data values

$x_2x_3 \ldots\ldots\ldots\ldots\ldots\ldots\ldots\ldots\ldots\ldots\ldots\ldots x_n$
$x_1x_2x_3 \ldots\ldots\ldots\ldots\ldots\ldots\ldots\ldots\ldots\ldots\ldots x_{n-1}$

Table 1
The sample ACF and PACF along with the *Box-Ljung Statistic*

Lag	*Autocorrelation*	*Partial autocorrelation function*	*Box-Ljung Statistic*	
			Value	df
1	0.631	0.631	49.846	1
2	0.359	−0.067	66.063	2
3	0.228	0.048	72.670	3
4	0.163	0.024	76.088	4
5	0.056	−0.098	76.495	5
6	−0.154	−0.257	79.568	6
7	−0.130	0.162	81.783	7
8	0.058	0.246	82.230	8
9	0.185	0.113	86.814	9
10	0.211	0.052	92.854	10
11	0.247	0.106	101.163	11
12	0.315	0.025	114.807	12
13	0.286	−0.079	126.147	13
14	0.159	−0.027	129.693	14
15	0.025	−0.018	129.784	15
16	0.006	0.061	129.790	16
17	0.036	0.084	129.974	17
18	−0.048	−0.105	130.315	18
19	−0.055	0.029	130.765	19
20	−0.010	−0.044	130.780	20
21	0.066	−0.034	131.442	21
22	0.056	−0.084	131.921	22
23	−0.002	−0.002	131.922	23
24	−0.054	−0.126	132.365	24
25	−0.110	−0.142	134.237	25
26	−0.137	−0.004	137.215	26
27	−0.170	0.005	141.798	27
28	−0.159	−0.014	145.890	28
29	−0.115	0.010	148.028	29
30	−0.047	0.058	148.384	30

Autocorrelation of order k implies the correlation between a set of data values and another set of data of the same size, but lagged by k time steps. For example lag-1 autocorrelation from the data series $\{x_1x_2x_3 \ldots\ldots\ldots\ldots\ldots\ldots\ldots\ldots\ldots\ldots\ldots\ldots x_n\}$ would be computed from the following boxed data pairs:

That is, the data pairs would be (x_1, x_2), (x_2, x_3), (x_3, x_4) etc. Knowledge of the autocorrelation function also aids in selecting time series models, such as autoregressive moving average (ARMA), autoregressive integrated average model (ARIMA), and so on and allows for the correct application of statistical methods in data analysis by aiding in the determination of whether the data are independent [21,33].

The lag-1 autocorrelation is the most commonly computed measure of persistence, but it is also sometimes of interest to compute autocorrelations at longer lags. Conceptually, this is no more difficult than the procedure for the lag-1 autocorrelation, and computationally the only difference is that the two series are shifted by more than one time unit. As a time series is shifted increasingly relative to itself, there is progressively less overlapping data to work with [33].

The collection of autocorrelations computed for various lags are called the autocorrelation function. Often autocorrelation functions are displayed graphically with the autocorrelations plotted as a function of lag. Applications of autocorrelation in geophysical studies are well-known [4,8,13,17,21,31,35].

In the present work, the maximum tsunami wave height time series are considered whose entries are obtained at 10-minute intervals. The data points contain 132 entries. In Table 1, the sample autocorrelation coefficients and the partial autocorrelation coefficients are presented along with the Box-Ljung statistic. The autocorrelation

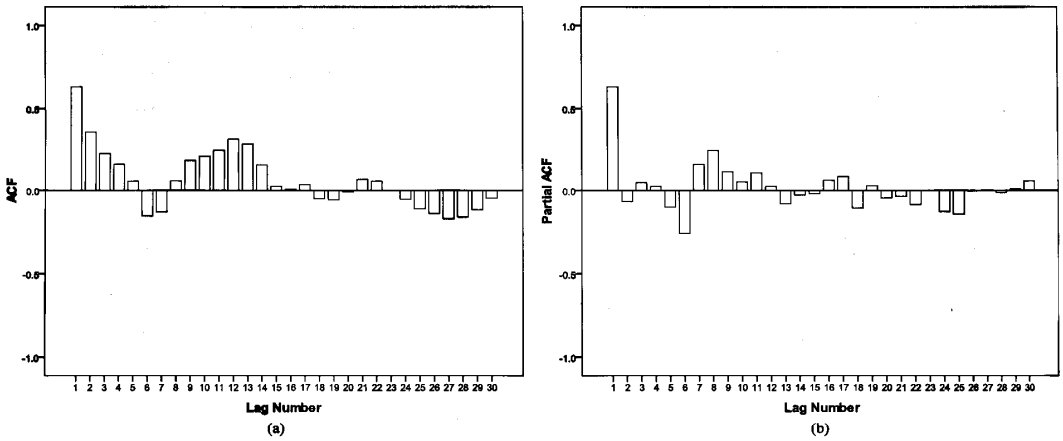

Fig. 1. a. Schematic showing the autocorrelation function (ACF) of maximum Tsunami wave height. b. Schematic showing the partial autocorrelation function (PACF) of maximum Tsunami wave height.

function is computed up to 30 lags. It has been observed that the lag-1 autocorrelation coefficient is high (> 0.5), which indicates that the maximum wave heights influence the subsequent wave heights in 10 minutes intervals. It should be noted that the autocorrelation coefficients are significant at 5% level. However, at higher lags, the autocorrelation coefficients are not high and the autocorrelation function does not tend to 0 with increase in the lags. Furthermore, the autocorrelation function has no sinusoidal pattern, although there are positive as well as negative spikes in the autocorrelation function. Therefore, the time series is not characterized by any cyclic pattern. The sample autocorrelation function and the sample partial autocorrelation function are displayed in Figs 1a and 1b.

3. Methodology

3.1. *Autoregression (AR)*

An autoregressive process of order p is denoted as AR(p) and is given by the equation [3]

$$\tilde{z}_t = \phi_1 \tilde{z}_{t-1} + \phi_2 \tilde{z}_{t-2} + \ldots + \phi_p \tilde{z}_{t-p} + a_t \tag{1}$$

where $\phi_1, \phi_2, \ldots, \phi_p$ are adjustable parameters and $\tilde{z}_t = z_t - \mu$ [3]. The autocorrelation function satisfies the equation

$$\rho_k = \phi_1 \rho_{k-1} + \phi_2 \rho_{k-2} + \ldots + \phi_p \rho_p \tag{2}$$

Substituting $k = 1, 2, \ldots, p$ in Eq. (2), the system of Yule-Walker equations is obtained [3]:

$$\begin{aligned} \rho_1 &= \phi_1 + \phi_2 \rho_1 + \ldots + \phi_p \rho_{p-1} \\ \rho_2 &= \phi_1 \rho_1 + \phi_2 + \ldots + \phi_p \rho_{p-2} \\ &\vdots \\ \rho_p &= \phi_1 \rho_{p-1} + \phi_2 \rho_{p-2} + \ldots + \phi_p \end{aligned} \tag{3}$$

The Yule-Walker estimates of the autoregressive parameters $\phi_1, \phi_2, \ldots, \phi_p$ are obtained by replacing the theoretical autocorrelation ρ_k by the estimated autocorrelation r_k. Thus, the matrix notation, the autoregression parameters can be written as:

$$\Phi = R^{-1} r \tag{4}$$

Where,

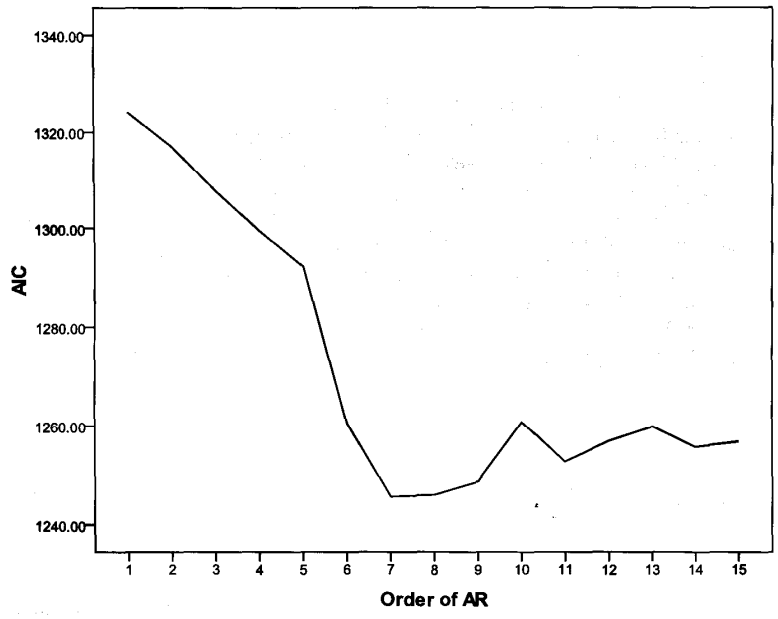

Fig. 2. Schematic showing the AIC for the competitive orders of autoregressive processes.

$$\Phi = \begin{bmatrix} \phi_1 \\ \phi_2 \\ \vdots \\ \phi_p \end{bmatrix}, r = \begin{bmatrix} r_1 \\ r_2 \\ \vdots \\ r_p \end{bmatrix} \text{ and } R = \begin{bmatrix} 1 & r_1 & r_2 & \cdots & r_{p-1} \\ r_1 & 1 & r_1 & \cdots & r_{p-2} \\ \vdots & \vdots & \vdots & \cdots & \vdots \\ r_{p-1} & r_{p-2} & r_{p-3} & \cdots & 1 \end{bmatrix} \tag{5}$$

The fifteen autoregressive models (AR(1), AR(2), ..., AR(15)) have been generated for tsunami maximum wave height time series, which has already been identified as a stationary time series using the method explained above. While developing the above autoregressive models, the Pearson correlations are computed between the actual and predicted values and the Akaike Information Criteria (AIC) corresponding to the models [33]. The results showed that the Pearson correlations are gradually increasing with an increase in the order of the autoregression. However, after order 7, the correlations are becoming almost constant despite increase in the order of the autoregressive model. It is therefore understood that the increase in the order after AR(7) is not having any significant impact upon the prediction. Therefore, it is concluded that seven previous values of the time series are having impact upon the eighth entry of the time series. Simultaneously, it has been observed that AIC of AR(7) attains its minimum for the seventh order of autoregression in Fig. 2. In the subsequent sections, seven previous values of the time series will be used to predict the eighth entry.

3.2. *Autoregressive integrated moving average (ARIMA)*

In Eq. (1), if we take $p = 1$, we get the AR(1) process whose parameters are obtained using the method described in the last section. From the AR(1) process, the characteristic root is obtained as 1.56, which is outside the unit circle. Thus, the time series is identified as non-stationary [5]. Consequently, ARIMA, a non-stationary process is used. A mixed autoregressive moving average (ARMA) model is expressed as [3]:

$$\phi(B)\,\tilde{z}_t = \theta(B)\,a_t \tag{6}$$

where $\phi(B)$ and $\theta(B)$ are polynomials of degree p and q respectively, B is the backward shift operator, and $\tilde{z}_t = z_t - \mu$. The ARMA process is stationary if the roots of $\phi(B) = 0$ lie outside the unit circle and it exhibits

explosive non-stationary behaviour if they lie inside the unit circle. If $\phi(B)$ is a stationary autoregressive operator, then the autoregressive integrated moving average (ARIMA) process is derived as

$$\phi(B)(1-B)^d \tilde{z}_t = \theta(B)\, a_t \tag{7}$$

Where, d denotes the number of times the stationary process is summed. Introducing the backward difference operator $\nabla = 1 - B$, and $\nabla^d \bar{z}_t = \nabla^d z_t$ the above equation becomes

$$\phi(B)\nabla^d \tilde{z}_t = \theta(B)\, a_t \tag{8}$$

where, considering the various values of p, d and q, the ARIMA model is written as ARIMA(p, d, q). In the cases of non-seasonal time series, values of p, d and q are rarely greater than 2 and the following orders of ARIMA are of most frequent use [3]:

• ARIMA(1,1,1)

In this case, Eq. (8) takes the form

$$(1-\phi_1 B)\nabla z_t = (1-\theta_1 B)\, a_t \tag{9}$$

• ARIMA(0,1,1)

In this case, Eq. (8) takes the form

$$\nabla z_t = (1-\theta_1 B)\, a_t \tag{10}$$

3.3. Autoregressive neural network (AR-NN)

The present paper applies artificial neural network (ANN) in the form of multilayer perceptron (MLP). Neural network models in artificial intelligence are usually referred to as artificial neural networks (ANNs); these are essentially simple mathematical models defining a function $f : X \rightarrow Y$ or a distribution over X or both X and Y, but sometimes models also intimately associated with a particular learning algorithm or learning rule. A common use of the phrase ANN model really means the definition of a class of such functions, where members of the class are obtained by varying parameters, connection weights, or specifics of the architecture such as the number of neurons or their connectivity. ANN is useful in the situations, where underlying processes / relationships may display chaotic properties. ANN does not require any prior knowledge of the system under consideration and are well suited to model dynamic systems on a real-time basis. An artificial neural network is a multiprocessor computer system based on the parallel architecture of the brain [14]. The advent of the feed forward ANN, or Multilayer Perceptron (MLP) with Backpropagation learning – an adaptation of the steepest descent method, opened up new avenues for the application of ANN for problems of practical interest [11]. In MLP, each network consists of several simple processors called neurons, or cells, which are highly interconnected and are arranged in several layers [11]. There are three basic types of layers: input layer, hidden layer(s), and output layer.

The theoretical details of MLP are available in various texts on ANN [14]; its suitability in thunderstorm atmospheric, environmental and oceanic modeling is known [11]. An equivalent form of the linear autoregressive model of order p given in Eq. (1) can be expressed as a fixed number of previous values of a time series including a noise term as follows:

$$x(t) = \sum_{i=1}^{p} \alpha_i x(t-i) + \in (t) \tag{11}$$

The above form is taken to show the resemblance between regression and ANN based forecast model. In Eq. (11), a linear function F^L can be introduced and its equivalent form would be [9]

$$x(t) = F^L(x(t-1), x(t-2), \ldots, x(t-p)) + \in (t) \tag{12}$$

In Eq. (12), if L is replaced by MLP, then an autoregressive neural network (AR-NN) model will be obtained. To develop the AR-NN model, seven predictors have been used. The predictors are coming from the time series itself. For example, if the time series is written as the sequence $\{x_t | t = 1, 2, \ldots, 132\}$, for the predictand x_8, the predictors are $x_1, x_2, x_3, x_4, x_5, x_6$, and x_7. It should be noted that the word 'predictand' stands for the dependent variable in any regressive model [33]. Since seven consecutive values are predicting the eighth value, finally, the

input matrix for the AR-NN would be of order (124×7) and the target output matrix would be of order (124×1). The entire set of 124 patterns has been divided into training and test cases in the ratio of 7:3. Training set means the set of data used to train the ANN and test set means the set of data used to test the goodness of the model [23]

The type of nonlinearity of an ANN is determined by the activation function. The theoretical details of activation function and its applications are available in Rojas [23]. There are different types of activation function available in the literature such as sigmoid function, tanh, etc. [23]. Advantages of sigmoid function are established [11]. This function is given by $f(x) = (1 + e^{-x})^{-1}$. In the present paper, sigmoid non-linearity is used to train the ANN. In mathematical form, the adaptive procedure of a feed forward MLP can be presented as

$$w_{k+1} = w_k + \eta d_k \tag{13}$$

The above equation represents an iterative process that finds the optimal weight vector by adapting the initial weight vector w_0. This adaptation is performed by presenting to the network pairs of input and target vectors in sequence. The direction vector d_k is the negative gradient of the output error function E. Mathematically, it is denoted as

$$d_k = -\nabla E(w_k) \tag{14}$$

Several methods have been proposed to speed-up the conventional backpropagation learning. In the present paper, the procedure of adaptive gradient learning proposed by Amari et al. [1] is adopted to train the MLP. An extensive description of the adaptive gradient learning is available [1]. Minimization of the mean squared error is chosen as the stopping criterion. The model has been validated over the entire set of 124 patterns. The results are discussed in the subsequent sections.

4. Evaluation of the models

In the present section, performances of the models are assessed statistically using the following statistics:

a. Percentage of Prediction error (PE)
b. Pearson correlation coefficient between actual and predicted values (PCC)
c. Willmott's index of order 1 (d)
d. Willmott's index of order 2 (d^2)

Overall prediction error (PE) is computed as [20]

$$PE = \frac{\langle |y_{predicted} - y_{actual}| \rangle \times 100}{\langle y_{actual} \rangle} \tag{15}$$

The PCC measures the degree of linear association between two variables. Mathematically it is written as [33]

$$\rho_{xy} = \frac{\text{Covariance}(x, y)}{\sigma_x \sigma_y} \tag{16}$$

Willmott [34] recommended computation of some 'summary measures' to assess the degree to which a model output fits an observed dataset. According to Willmott, these measures are more illuminating than the measure of coefficient of determination and correlation [6,7]. Fox [10] recommended the use of mean square error (MSE) but Willmott [34] described the limitations of the MSE, and alternatively proposed and used as 'index of agreement' of the form

$$d^{\alpha} = 1 - \left[\sum_i |P_i - O_i|^{\alpha}\right] \left[\sum_i \left(|P_i - \bar{O}| + |O_i - \bar{O}|\right)^{\alpha}\right]^{-1} \tag{17}$$

where $\alpha = 1$ and 2, P implies predicted value, and O implies observed value. For $\alpha = 1$ and $\alpha = 2$, one can get d and d^2. Closeness of Willmott's indices to 1 implies good predictive model.

Among all the models under study, the minimum PE and maximum PCC occurs in the case of AR-NN. However, in the other models PE and PCC are sufficiently high. The values can be observed in Fig. 3. In the next step, the values

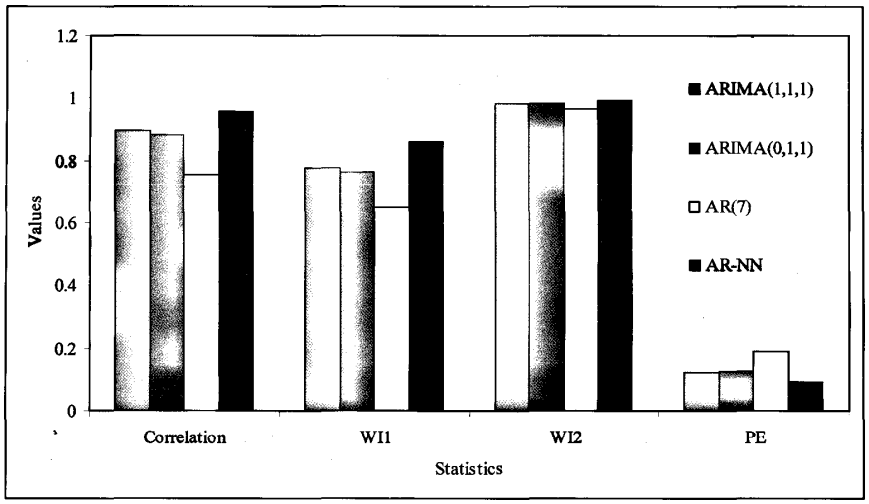

Fig. 3. Schematic showing the Prediction Error, Pearson Correlation, Willmott's indices of order 1 (WI1) and order 2 (WI2) available for the AR(7), ARIMA(1,1,1), ARIMA(0,1,1) and AR-NN models.

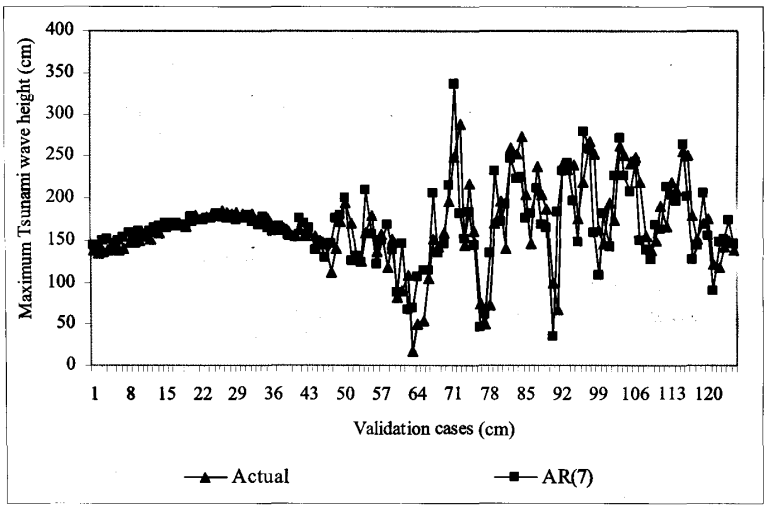

Fig. 4. Schematic showing the association between the actual maximum tsunami wave height and those predicted by AR(7).

of the WI are compared for the entire model under study. It is observed that in case of AR-NN, the value is greater than 0.8 and in the case of AR(7) the value is 0.65 which is the minimum WI(1). ARIMA(1,1,1) and ARIMA(0,1,1) have WI(1) values very close to each other. Similar trend is observed in the case of WI(2) which attains its maximum for AR-NN and minimum for AR(7). This indicates that AR(7) has the least potential to predict the time series of maximum tsunami wave height. Although ARIMA(1,1,1) and ARIMA(0,1,1) are sufficiently capable of modeling the time series, AR-NN performed better with the same set of seven predictors. Therefore, it is understood that AR-NN of order seven is the best model for the maximum tsunami wave height time series. In Figs 4,5, 6 and 7, the line diagrams for the actual time series and those predicted by AR(7), ARIMA(1,1,1), ARIMA(0,1,1) and AR-NN respectively are presented. All the models exhibit the random nature of the time series. However, it is observed in

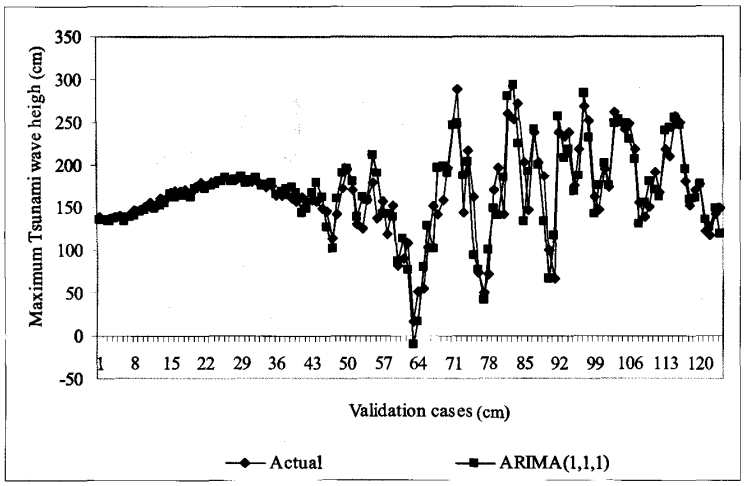

Fig. 5. Schematic showing the association between the actual maximum tsunami wave height and those predicted by ARIMA(1,1,1).

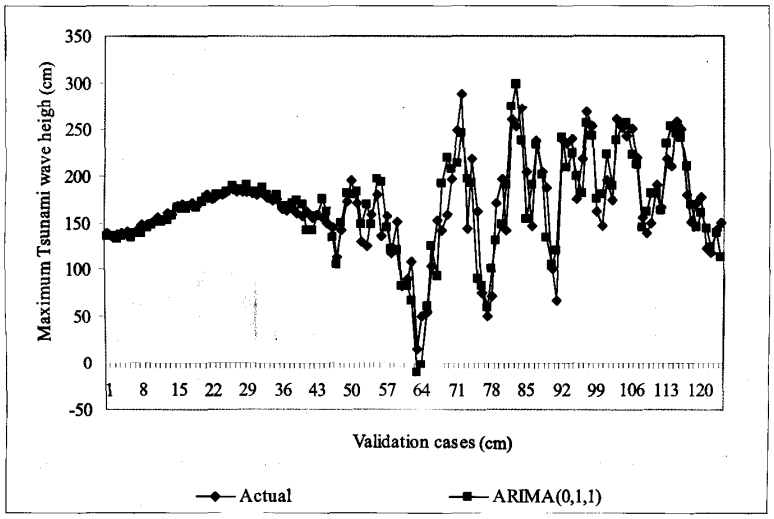

Fig. 6. Schematic showing the association between the actual maximum tsunami wave height and those predicted by ARIMA(0,1,1).

Fig. 7 that the maximum closeness between actual and predicted time series occurs in the case of AR-NN with seven previous values as predictors. In Fig. 8, the prediction is presented. First, 5% error of prediction is chosen as the upper limit of acceptable error. It is found that in 33.87% of the validation cases, the prediction error is less than 5% for the AR(7). Thus, prediction yield in this case is 0.3387. It has been found that the maximum prediction yield for 5% error in the case of AR-NN, is 0.5806. Similarly, in the case of 10% allowable prediction error, the maximum prediction is 0.8145, which corresponds to AR-NN. These prediction yields the supremacy of AR-NN model over the other models. As a further visual support to the prediction quality for the models under consideration, the residuals corresponding to each model calculated over the entire validation set are presented in Fig. 9, which shows that the residuals corresponding to AR-NN model lies below the other competitive models in most of the validation cases.

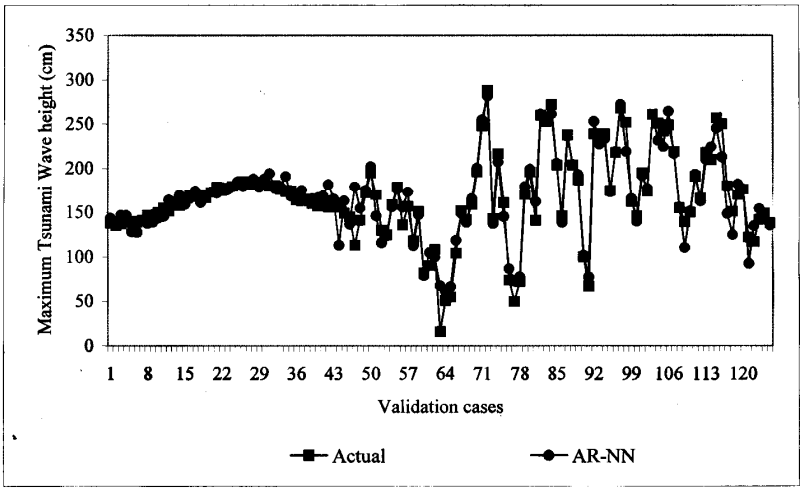

Fig. 7. Schematic showing the association between the actual maximum tsunami wave height and those predicted by AR-NN with seven predictors.

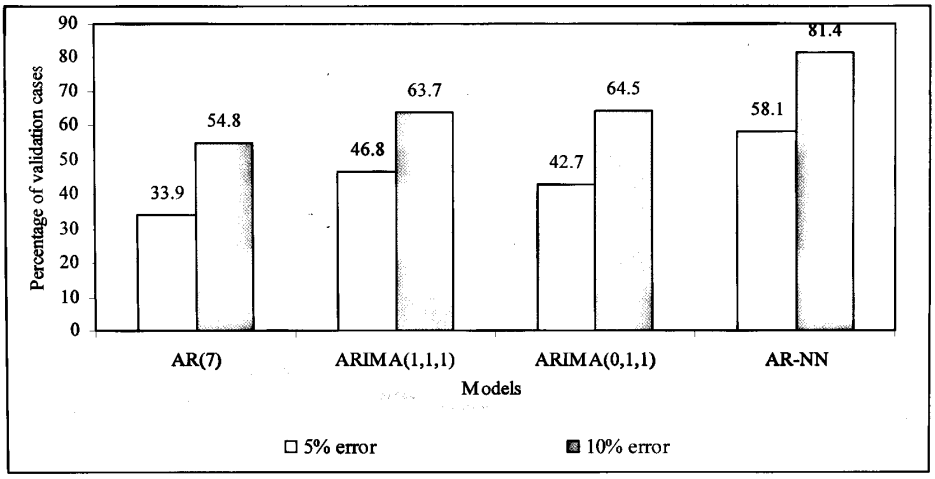

Fig. 8. Schematic showing the percentage of test cases where AR(7), ARIMA(1,1,1), ARIMA(0,1,1) and AR-NN models produce prediction errors 5% and 10% respectively.

In the study demonstrated above we have restricted the ARIMA models to the orders of (1,1,1) and (0,1,1). The natural question that may arise is: *Why are we not experimenting with higher orders of ARIMA*? It is already stated that the theoretical reasons behind these popular choices of orders of ARIMA are available in reference [3]. The computation in this study shows that these two orders are generating predictions which are having very high correlation coefficients, high Willmott's indices and very low error of prediction. Thus, adding any more order of autoregression or moving average to this model would add nothing but some degree of complexity. That is why, the orders of ARIMA are not increased further.

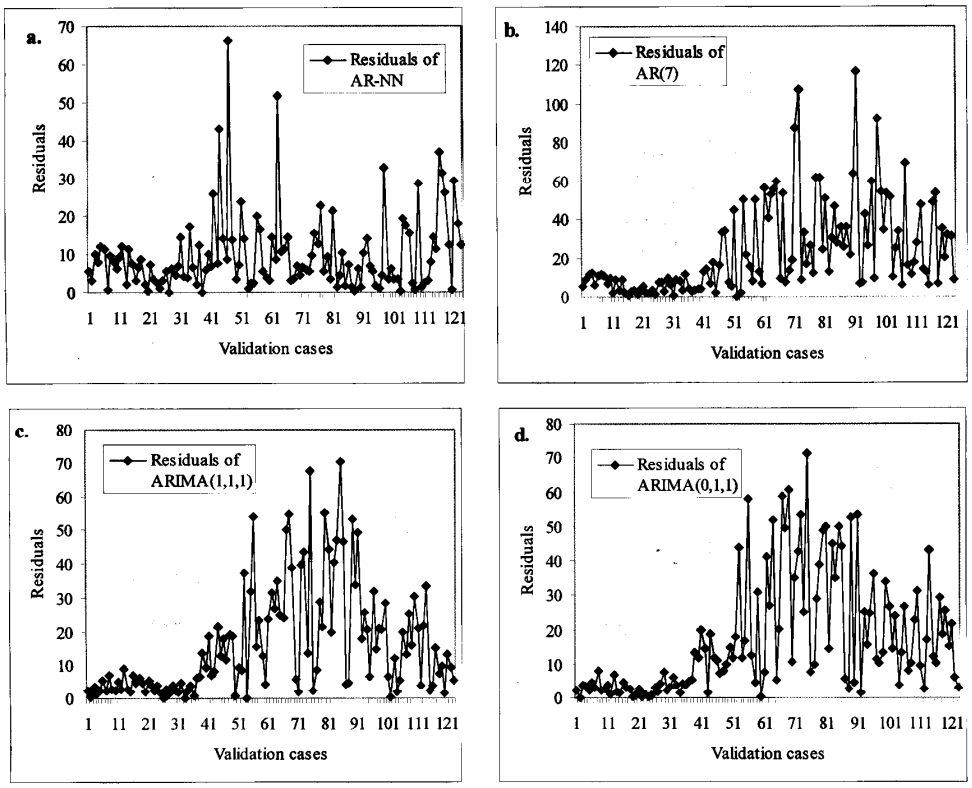

Fig. 9. Schematics showing the residuals for the predictions from (a.)AR-NN, (b)AR(7), (c)ARIMA(1,1,1), and (d) ARIMA(0,1,1).

5. Conclusion

In the present paper, a univariate approach is adopted to predict the maximum tsunami wave height over Sibolga, Sumatra. Initially, the autocorrelation structure is analyzed and it is revealed that there is no deterministic pattern in the time series and the time series is not generated by a stationary process. In the next step, AR(7) model is generated for the said time series. After considering the model, it is shown that AR(7) produces the minimum values of Pearson correlation coefficient, Willmott's indices and maximum values of percentage of prediction error. In the next phase, ARIMA(1,1,1) and ARIMA(0,1,1) models are generated. In these models, Pearson correlation coefficient and Willmott's indices are very close to each other. The final model is the AR-NN model, which produces maximum correlation coefficient and Willmott's indices and minimum percentage of prediction error. Therefore, the final conclusion is that the AR-NN with seven predictors best fits the time series of maximum tsunami wave height over the study zone and that it has maximum prediction capacity among all the univariate models considered in this study.

References

[1] S. Amari, H. Park and K. Fukumkizu, Adaptive Method of Realizing Natural Gradient Learning for Multilayer Perceptrons, *Neural Computation* **12** (2000), 1399–1400.

[2] C.J. Ammon, C. Ji, H.K. Thio, D. Robinson, S. Ni, V. Hjorleifsdottir, H. Kanamori, T. Lay, S. Das, D. Helmberger, G. Ichinose, J. Polet and D. Wald, Rupture process of the 2004 Sumatra-Andaman earthquake, *Science* **308** (2005), 1133–1139.

[3] G.E.P. Box, G.M. Jenkins and G.C. Reinsel, *Time series analysis: Forecasting and control* (Third Edition), Dorling Kindersley (India) Pvt Ltd., licensees of Pearson Education in South Asia, New Delhi, India, 2007.
[4] A.C. Brett and S.E. Tuller, The Autocorrelation of Hourly Wind Speed Observations, *Journal of Applied Meteorology* **30** (1991), 823–833.
[5] J.L. Carrion-i-Silvestre, A. Sansó-i-Rosselló and M. Artís Ortuño, Unit root and stationarity tests' wedding, *Economics Letters* **70** (2001), 1–8.
[6] S. Chattopadhyay and G. Chattopadhyay, Comparative study among different neural net learning algorithms applied to rainfall time series, *Meteorological Applications* **15** (2008), 273–280.
[7] S. Chattopadhyay and G. Chattopadhyay-Bandyopadhyay, Artificial Neural network versus autoregressive approach: Prediction of total ozone time series, *Model Assisted Statistics and Applications* **2** (2007), 107–120.
[8] P.C. Chu, W. Guihua and Y. Chen, Japan Sea Thermohaline Structure and Circulation. Part III: Autocorrelation Functions, *Journal of Physical Oceanography* **32** (2002), 3596–3615.
[9] G. Dorffner, Neural network for time series processing, *Neural Network World* **6** (1996), 447–468.
[10] D.G. Fox, Judging air quality model performance: a summary of the AMS workshop on Dispersion Model Performance, *Bulletin of American Meteorological Society* **62** (1981), 599—609.
[11] M. W. Gardner and S. R. Dorling, Artificial neural networks: the multiplayer perceptron: a review of applications in atmospheric sciences, *Atmospheric Environment* **32** (1998), 2627–2636.
[12] E.L. Geist, V.V. Titov, D. Arcas, F.F. Pollitz and S.L. Bilek, Implications of the 26 December 2004 Sumatra–Andaman Earthquake on tsunami Forecast and Assessment Models for Great Subduction-Zone Earthquakes, *Bulletin of the Seismological Society of America* [online] **97**(1A) (2007), S249–S270, doi:10.1785/0120050619.
[13] D.S. Gutzler and K.C. Mo, Autocorrelation of Northern Hemisphere Geopotential Heights, *Monthly Weather Review* **111** (1983), 155–164.
[14] S. Haykin, *Neural Networks: A Comprehensive Foundation* (*Second edition*), Pearson Education Inc., New Delhi, India, 2001.
[15] L.-S. Hwang and D. Divoky, Tsunami Generation, *Journal of Geophysical Research* **75** (1970), 6802–6817.
[16] B.E. Jaffe, J.C. Borrero, G.S. Prasetya, R. Peters, B. McAdoo, G. Gelfenbaum, R. Morton, P. Ruggiero, B. Higman, L. Dengler, R. Hidayat, E. Kingsley, W. Kongko, Lukijanto, A. Moore, V.V. Titov and E. Yulianto, Northwest Sumatra and Offshore Islands Field Survey after the December 2004 Indian Ocean Tsunami, *Earthquake Spectra* **22**(S3) (2006), S105–S135.
[17] V.M. Melnikov and D.S. Zrnić, Autocorrelation and Cross-Correlation Estimators of Polarimetric Variables, *Journal of Atmospheric and Oceanic Technology* **24** (2007), 1337–1350.
[18] H.O. Mofjeld, F.I. González, V.V. Titov, A.J. Venturato and J.C. Newman, Effects of Tides on Maximum Tsunami Wave Heights: Probability Distributions, *J Atmos Oceanic Technol* **24** (2007), 117–123.
[19] H.O. Mofjeld, F.I. Gonz'alez, E.N. Bernard and J.C. Newman, Forecasting the Heights of Later Waves in Pacific-Wide Tsunamis, *Natural Hazards* **22** (2000), 71–89.
[20] P. Perez, A. Trier and J. Reyes, Prediction of PM2.5 concentrations several hours in advance using neural networks in Santiago, Chile, *Atmospheric Environment* **34** (2000), 1189–1196.
[21] I.A. Pérez, M. García, M.L. Sánchez and B. de Torre, Autocorrelation Analysis of Meteorological Data from a RASS Sodar, *Journal of Applied Meteorology* **43** (2004), 1213–1223.
[22] N.T. Puspito and I. Gunawan, Tsunami sources in the Sumatra region, Indonesia and Simulation of the 26 December 2004 Aceh Tsunami, *ISET Journal of Earthquake Technology* **42** (2005), 111–125.
[23] R. Rojas, *Neural Networks*, Springer-Verlag, Berlin, 1996.
[24] K. Satake, T.T. Aung, Y. Sawai, Y. Okamura, K.S. Win, W. Swe, C. Swe, T.L. Swe, S.T. Tun, M.M. Soe, T.Z. Oo and S.H. Zaw, Tsunami heights and damage along the Myanmar coast from the December 2004 Sumatra-Andaman earthquake, *Earth Planets Space* **58** (2005), 243–252.
[25] N. Saxena and A. Zielinski, Deep-ocean system to measure tsunami wave-height, *Marine Geodesy* **5** (1981), 55–62.
[26] L. Tang, V.V. Titov and C.D. Chamberlin, Development, testing, and applications of site-specific tsunami inundation models for real-time forecasting, *Journal of Geophysical Research* [online] **114** (2009), C12025, doi:10.1029/2009JC005476.
[27] Y. Tanioka and K. Satake, Tsunami generation by horizontal displacement of ocean bottom, *Geophysical Research Letters* **23** (1996), 861–864.
[28] V.V. Titov, A.B. Rabinovich, H.O. Mofjeld, R.E. Thomson and F.I. Gonz'alez, The Global Reach of the 26 December 2004 Sumatra Tsunami, *Science* **309** (2005), 2045–2048.
[29] V.V. Titov, F.I. Gonz'alez, E.N. Bernard, M.C. Eble, H.O. Mofjeld, J.C. Newman and A.J. Venturato, *Real-Time Tsunami Forecasting: Challenges and Solutions*, Kluwer Academic Publishers, Netherlands, 2003.
[30] Y. Tsuji, Y. Namegaya, H. Matsumoto, S.I. Iwasaki, W. Kanbua, M. Sriwichai and V. Meesuk, The 2004 Indian Tsunami in Thailand: Surveyed runup heights and tide gauge records, *Earth Planets Space* **58** (2006), 223–232.
[31] X.L. Wang, Accounting for Autocorrelation in Detecting Mean Shifts in Climate Data Series Using the Penalized Maximal t or F Test, *Journal of Applied Meteorology and Climatology* **47** (2008), 2423–2444.
[32] J.J. Wijetunge, Tsunami on 26 December 2004: Spatial Distribution of Tsunami Height and the Extent of Inundation in Sri Lanka, *Science of Tsunami Hazards* **24** (2006), 225–239.
[33] D.S. Wilks, *Statistical Methods in Atmospheric Sciences*, Second Edition, Elsevier Inc., UK, 2006.
[34] C.J. Willmott, Some comments on the evaluation of model performance, *Bulletin of American Meteorological Society* **63** (1982), 1309–1313.
[35] D.P. Wylie, B.B. Hinton, M.R. Howland and R.J. Lord, Autocorrelation of Wind Observations, *Monthly Weather Review* **113** (1985), 849–857.